*Terra Antartica*
2001, 8(4), 491-505

# Statistical Analysis of Wireline Logging Data of the CRP-3 Drillhole (Victoria Land Basin, Antarctica)

C.J. BÜCKER[1§*], R.D. JARRARD[2], F. NIESSEN[3] & T. WONIK[1]

[1]GGA, Leibniz Institute for Applied Geosciences, Stilleweg 2, 30655 Hannover - Germany
[2]Dept. of Geology & Geophysics, 717 WBB, Univ. of Utah, Salt Lake City, UT 84112-0111 - USA
[3]Alfred Wegener Institut für Polar- und Meeresforschung, Columbusplatz, 28575 Bremerhaven - Germany
[§]Present address: RWE-DEA AG, Ueberseering 40, 22297 Hamburg - Germany

*Received* 16 January 2001; *accepted in revised form* 13 November 2001

**Abstract** - Drillhole CRP-3 in northern McMurdo Sound (Ross Sea, Antarctica) targeted the western margin of the Victoria Land basin to investigate Neogene to Palaeogene climate and tectonic history by obtaining continuous core and downhole logs. Well logging of CRP-3 has provided a complete and comprehensive data set of *in situ* geophysical measurements down to nearly the bottom of the hole (920 m below sea floor (mbsf)).

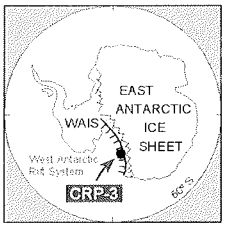


This paper describes the evaluation and interpretation of the downhole logging data using the multivariate statistical methods of factor and cluster analysis. The factor logs mirror the basic geological controls (*i.e.*, grain size, porosity, clay mineralogy) behind the measured geophysical properties, thereby making them easier to interpret geologically. Cluster analysis of the logs delineates individual logging or sedimentological units with similar downhole geophysical properties. These objectively and independently defined units help differentiate lithological and sedimentological characteristics (*e.g.* grain size, sediment provenance, glacial influence).
For CRP-3, the three factor logs derived from the downhole measurements reflect sediment grain size (proxy for lithology), the occurrence of diamict and/or conglomerate (glacial influence), and sediment provenance.
It is possible to divide the borehole into three main sections on the basis of cluster analysis of the three factor logs. The top section down to about 200 mbsf is dominated by mudstone with clearly different physical properties from the mudstones occurring below this depth. Beneath 200 mbsf sandstones dominate the lithology. Two types of sandstones were characterised in the early Oligocene/late Eocene sequence, with a division between the two types occurring at about 630 mbsf. These two types of sandstones, which are differentiated mainly on the basis of their magnetic and radiogenic properties, can be correlated by detrital mode provenance analysis. Comparison of the results of the factor and cluster analyses with the reflection seismic profiles shows that the major change in sediment source from the Victoria Group to the Taylor Group at 630 mbsf (earliest Oligocene) is not seen by seismic sequence analysis. This observation may have important consequences for the entire Ross Sea seismic stratigraphy.

## INTRODUCTION

The Cape Roberts Project (CRP) was designed to document past variations in Antarctic ice cover and climate and to reconstruct the early uplift history of the nearby Transantarctic Mountains (TAM). In austral spring 1999, the third and final drillhole (CRP-3) of the Cape Roberts Project was successfully completed. The three CRP drillholes CRP-1, CRP-2/2A, and CRP-3 are located in a sedimentary basin about 20 km offshore from Cape Roberts, which gave the name for the project. A detailed description of the project, the geological and time setting, and preliminary results, together with a lithology profile, have been published by the Cape Roberts Science Team (1998, 1999, 2000). At a water depth of 299.7 m, drillhole CRP-3 reached a final depth of 939.4 m below sea floor (mbsf). All of the downhole logging tools were run almost to the bottom of the hole. The downhole logs are essential to achieve the aims of the project, in particular in linking seismic reflection data to the drillhole geology and for seismic sequence analysis. This paper describes the interpretation of the downhole logs and the relationship to geological, sedimentary and seismic results. Downhole logging in CRP-3 was undertaken in four phases depending on the drilling progress. The first two phases were carried out after drilling to a depth of 346 mbsf with an HQ drillstring (96 mm diameter). Due to a fault zone at 257 – 261 mbsf, the hole was logged down to 346 mbsf first with the drillstring above 261 mbsf. Then the drillstring was pulled up and the upper part logged. After this second phase of logging, the HQ drillstring was cemented and drilling continued with an NQ drillstring (76 mm diameter). The third phase of logging was conducted

*Corresponding author (christian.buecker@rwedea.de)

when NQ coring had reached 774 mbsf. The fourth and final phase of logging was undertaken when NQ coring reached the final total depth for CRP-3, 939.42 mbsf. Except for the temperature logs, all of the logs were recorded only while the tool was hoisted from the bottom of the hole.

The downhole logging tools used in CRP-3 are the same as those used in CRP-2/2A (Cape Roberts Science Team, 1999), with some additional tools. A detailed description of the logging tools and techniques is given in the Initial Report on CRP-3 (Cape Roberts Science Team, 2000). A total of 9 tools were used, yielding values for 15 physical and chemical parameters. Additionally to these conventional downhole tools, a borehole televiewer (BHTV) was run and a vertical seismic profiling (VSP) experiment with two offset measurements was carried out. BHTV and VSP results are presented by Jarrard et al. (this volume) and by Henrys et al. (this volume), respectively. Downhole temperature profiles were collected several times; the results are published by Bücker et al. (this volume).

Each logging phase consisted of running the following logging tools: temperature (first and last run of each phase), spectral gamma ray (K, Th, U), dual laterolog (deep and shallow resistivity), magnetic susceptibility, array induction (resistivity at four penetration depths), neutron porosity, borehole televiewer (with magnetic field measurements), sonic velocity, dipmeter (with magnetic field measurements), vertical seismic profile. In addition to this standard suite of CRP-3 downhole measurements, the fourth phase included a density log over the entire drillhole and offset vertical seismic profiling.

The downhole measurements were interpreted using multivariate statistics in a similar approach to that used in CRP-2/2A (Bücker et al., 2000b). The application of multivariate statistical tools proved to be very quick, objective and reliable and resulted in a new integrated presentation of logs. Factor and cluster analyses are excellent methods for handling a large amount of logging data and meeting the demand for a fast, reliable and objective evaluation and interpretation. Again, as for CRP-2/2A, factor analysis was used to rescale and reduce the original data set, and cluster analysis was used to block log data and define sedimentological characteristics such as grain size and provenance changes as objectively as possible.

## DOWNHOLE LOGGING DATA AND QUALITY CONTROL

A complete set of downhole logs was recorded in CRP-3 using tools from the Leibniz Institute for Applied Geosciences (GGA-Institut, Germany). All of these tools were manufactured by ANTARES GmbH (Bremen, Germany) and are slimhole tools with a diameter of not more than 52 mm. They can be compared to commercial wireline logging tools (*e.g.*, Schlumberger, Western Atlas). A description of the measurement principles and techniques has been published by the Cape Roberts Science Team (1999, 2000). Comparisons with the results of the core measurements and cross correlations show the data to be of generally good quality.

Sample interval, radius of investigation, vertical resolution and a summary of tool responses of each logging tool have been published by the Cape Roberts Science Team (2000). Figure 1 shows a composite plot of all downhole measurements used in this study, together with a simplified lithological log derived by visual core descriptions (Cape Roberts Science Team, 2000). Depth shifts of as much as 1 m can occur among different logging runs, caused mostly by cable stretch or slip. Prior to this presentation, all downhole logs were first matched to a reference log (electrical resistivity) and then to core depth, thus making downhole log and core measurements comparable even at a small scale. In general, depth offsets were less than a few decimetres, but sometimes up to one metre.

Log quality and reliability are judged to be excellent for nearly all of the CRP-3 logging tools except the sonic tool. This conclusion is based on internal consistency and calibration tests for some tools, replicability as observed in short intervals logged twice with the same tool (repeat sections), and similarity of log character among different logging tools that use different physical properties to detect the same geological variable. All the following descriptions of downhole logs refer to figure 1.

### BOREHOLE GEOMETRY

Borehole calliper was measured with the dipmeter tool, which uses the four resistivity pads as a four-arm calliper tool. Hole deviation was measured with dipmeter and televiewer tools, based on 3-axis fluxgate magnetometer and 2- or 3-axis accelerometer recordings. During all downhole measurements a magnetic field station was run on the ice to have a control for magnetic storms. This was important as the Cape Roberts drillhole location is close to the magnetic southpole. The four-arm calliper measurements together with the dip-angle of the inclination of the borehole are given in Figure 1. In general, the hole shows a good calliper with only a few larger breakouts and washouts, which do not exceed 250 mm. Calliper and dip-angle measurements could not be obtained in the fault zone at 255 – 275 mbsf where the drillstring was in place. Hole size had two effects on CRP-3 logging. First, a bridge, presumably due to sticky clays at the top and bottom of the volcanic intrusion at 900 mbsf, prevented the tools from reaching the bottom 18 – 39 m of the hole. Only the temperature tool, which was the first log run at this depth, reached 921 mbsf. To prevent

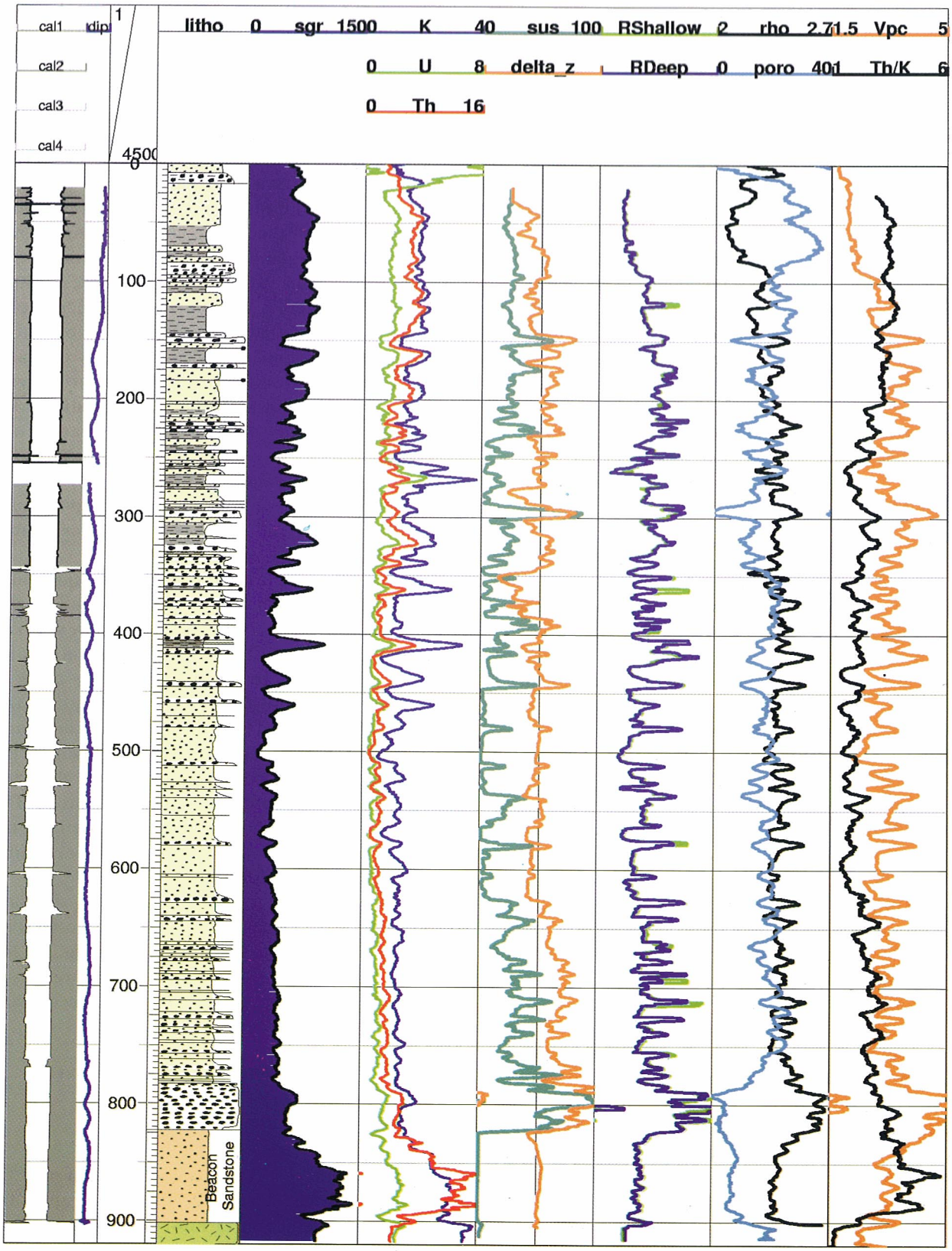


*Fig. 1* - Core derived lithology and downhole logs for hole CRP-3. From left to right, the following parameters are shown: first column: calliper of the borehole (cal1 – cal4); cal 1 and cal2 are the calliper logs for the HQ borehole (cal1 left part, 110 – 140 mm, cal2 right part 140 – 110 mm), cal3 and cal4 are the calliper logs for the NQ borehole (cal3 left part, 90 – 110 mm, cal4 right part, 110 – 90 mm); second column: angle of inclination of the borehole (0° (left)– 3°(right)); between second and third column: depth scale 1:4500 and depth in metres below sea floor; third column: core-derived lithology, legend see Barrett et al., (this volume) fourth column: spectral gamma ray log (sgr, 0 – 150 API); fifth column: potassium (K, 0 – 4 %), uranium (U, 0 – 8 ppm), thorium (Th, 0 – 16 ppm); sixth column: susceptibility log (sus, 0 – $100\times10^{-3}$ SI), anomaly of vertical component of magnetic field delta_z (-500 – 500 nT); seventh column: electrical resistivity log (RShallow, RDeep, 0.5 – 500 ohm·m), logarithmic scale; eighth column: density log (rho, 2.0 – 2.7 g/cm$^3$), porosity log (poro, 0 – 40 p.u.); ninth column: whole-core P-wave velocity (Vpc, 1.5 – 5.0 km/s), thorium/potassium ratio (Th/K, 1 – $6\times10^{-4}$) (for lithology legend, see Barrett et al., this volume).

tool losses, subsequent logging runs were stopped at shallower depths of 900 – 919 mbsf.

Second, an enlarged hole can degrade the accuracy of most log types. As can be seen in the overall good calliper log in figure 1, hole conditions are not a significant source of error for the CRP-3 logs. About a dozen washouts were detected in the dipmeter calliper log, most of them caused by unstable hole conditions associated with loose or unconsolidated sands.

Measured hole deviations are remarkably small. Over the entire borehole, the angle of inclination is less than 3°, in the lower part less than 2°, and sharp curve inflections were not observed. In the top 350 metres the hole deviation is 1.0° – 2.5° to the southwest, and about 1.5° to the southeast in the lower part of the hole. This means that the borehole is nearly vertical and the hole deviation does not have any influence on the downhole measurements.

## SPECTRAL GAMMA RAY

The spectral gamma ray tool was run down to 918 mbsf and reached the volcanic intrusion. Rare spikes caused by artefacts were observed on the raw gamma ray logs. These spikes resulted from noise-induced incorrect partitioning of the spectrum of gamma-ray energies and could be detected as a sharp positive spike in one elemental concentration and corresponding negative spike in one of the other two elemental concentrations. These spikes were edited and removed.

Gamma ray measurements were also made inside the drillstring (0 – 25 mbsf, 255 – 275 mbsf), and the attenuated values were corrected by using the ratio of the measurements inside and outside of the drillstring. No definite explanation can be given for the high uranium values in the Quaternary section of the borehole down to 20 mbsf. These may be attributed to a higher organic content.

Gamma ray values (from the spectral gamma ray log, sgr) and the potassium (K), thorium (Th), and uranium (U) contents show a general decrease downhole to the top of the doleritic shear zone at 790 mbsf. The highest sgr and thorium values were observed for the Beacon Sandstone in the depth section between 820 mbsf and 900 mbsf. The Beacon Sandstone can be divided into two sections mainly using the thorium log, which shows very high values in the lower part of the Beacon Sandstone below 850 mbsf. No other physical property shows a difference for different parts of the Beacon Sandstone. The difference in the thorium log may indicate different alteration stages.

In the uppermost part of the borehole, sgr shows more or less constantly high values up to 100 API although the lithology log shows alternating sandstones, mudstones and diamictites. The gamma ray log is traditionally used as a shale/sand indicator and to estimate shale content (Rider, 2000). However the expected distinction between mudstone and sandstone was not observed in the CRP-3 borehole above 120 mbsf. The high gamma ray values in this uppermost section of the borehole indicate a higher mud content in the sand and diamictite sections than the lithology log indicates. Below about 144 mbsf, the sgr log exhibits a good correlation with the lithological log, with high values for mudstones and low values for sandstones. The conglomerates do not show any extinct gamma ray values. Below about 460 mbsf the gamma ray data show the lowest values in the entire borehole, with only small fluctuations that clearly indicate sandstones. From about 630 mbsf to 790 mbsf the gamma ray values are fairly constant, with a slight increase towards the top of the dolerite shear zone at 790 mbsf. However, the traditionally expected gamma-ray pattern for coarse and fine-grained sediments is obscured in formations with immature unclean sands that contain substantial quantities of radioactive minerals, such as potassium feldspar and micas, and which contain a considerable amount of clay.

The overall pattern of the thorium/potassium ratio (Th/K, Fig. 1) within the Tertiary section of the borehole down to 790 mbsf indicates three petrophysical units. This ratio shows high and constant values down to 200 mbsf, and then drops to lower values varying from 200 to 630 mbsf, and below 630 mbsf the Th/K ratio is again high and varying. As the Th/K ratio is not influenced by the absolute radionuclide concentrations, these differing ratios may indicate different sediment sources. The broad pattern of downhole sgr variations reflects the combination of decreasing mud component and increasing Beacon sandstone source downhole.

Below 200 mbsf, changes in grain size are reflected in the sgr, and the tool can be used as a facies indicator. Due to this relationship, the sgr log shows a close correlation with the core-based palaeobathymetry curve (Cape Roberts Science Team, 2000).

## MAGNETIC SUSCEPTIBILITY AND ANOMALY OF THE VERTICAL INTENSITY OF THE MAGNETIC FIELD

The magnetic susceptibility tool was run over the entire borehole down to 902 mbsf. The gap in the fault zone from 255 to 275 mbsf was filled by cross correlation with downcore velocity measurements (correlation coefficient 0.65).

The most prominent feature of the susceptibility log (Fig. 1) relates to the Beacon Sandstone, which shows more or less zero susceptibility values and in some cases negative ones due to properties of pure quartz (quartz has a low negative susceptibility due to its diamagnetism). Delta_z, the anomaly of the vertical intensity of the magnetic field, also shows no

changes for the Beacon Sandstone section and thus indicates the Beacon Sandstone is effectively non-magnetic in the depth interval 820 – 900 mbsf. This is remarkable, because the sgr log shows clear differences within the Beacon Sandstone. The non-magnetic behaviour of the Beacon Sandstone may also provide new information for the interpretation of the aeromagnetic anomaly observed between the Cape Roberts drillhole locations and the coastline (Bozzo et al., 1997). This anomaly may be explained by an absence of the Beacon Sandstone in this region resulting in an unroofing of the underlying volcanic intrusion.

Grain size affects both the magnetic susceptibility and spectral gamma ray logs. Fine-grained sediments (mud, clay) often have much higher amounts of both magnetic and radiogenic minerals than coarse-grained sediments like sandstones (Bücker et al., 2000a). Therefore, the combination of sgr and susceptibility logs usually provides a robust indicator of sandstone versus shale. However, the susceptibility also shows a response to the conglomerates. Most of the conglomerates below 200 mbsf show a marked peak in susceptibility, indicating elevated magnetite content.

In most cases, changes in the magnetic anomaly value (delta_z) are closely related to susceptibility. The magnetic anomaly curve reflects the remanent and induced magnetism of the sediments and shows a higher vertical resolution in signal strength than the susceptibility curve, which responds only to the induced magnetisation. Remanence values can be calculated from the values of the magnetic field and susceptibility measurements and can be used to construct a more detailed magnetic anomaly model of the aeromagnetic anomaly west of the Cape Roberts drillsites (Bozzo et al., 1997).

The magnetic susceptibility and magnetic anomaly logs show a pattern similar to the gamma ray and thorium/potassium ratio logs. Susceptibility is uniformly high down to about 200 mbsf and uniformly low in the interval 444 – 630 mbsf. Below 630 mbsf down to 790 mbsf the susceptibility again shows high values. The zone from 200 to 444 mbsf shows an alternation between these two levels. The overall pattern in the magnetic susceptibility and magnetic anomaly logs, more than that of the gamma ray log, appear to be more closely related to provenance changes than to variations in grain size. Thus, the low susceptibility values in the depth section 200 – 630 mbsf indicate a mainly Beacon source, which consists of nonmagnetic sandstones.

Diamictites and conglomerates can be detected over the entire borehole section below 144 mbsf due to their enhanced susceptibility and magnetic anomaly values. This response is particularly characterized below 440 mbsf, where each conglomerate section and even relatively large lonestones were detected on the basis of susceptibility and magnetic anomaly variations.

## ELECTRICAL RESISTIVITY

Electrical resistivity shown in figure 1 was measured with the dual-laterolog tool, which gives a ten times higher vertical resolution than the array induction tool. The data gap in the fault zone from 255 to 275 mbsf was filled by cross correlation with core p-wave velocity (correlation coefficient 0.63). With the dual-laterolog, electrical resistivity was measured at two depths of investigation: "RDeep" and "RShallow". Both curves show a very high correlation, and differences in these two curves indicate rock fracture in this case where this is absence of invasion of a borehole fluid of anomalous resistivity.

Electrical resistivity mainly responds to formation porosity, as the pore fluids rather than the rock matrix affect electrical conductivity. Resistivity can also be influenced by clay minerals, and importantly clay effects depend on the salinity of the formation fluid. Clay conducts electricity, and thus decreases resistivity in low-porosity rocks (Waxman & Smits, 1968); on the other hand, clay increases tortuosity and therefore increases resistivity in high-porosity rocks (Erickson & Jarrard, 1998). However, clay mineral concentration in CRP-3 is low (Neumann & Ehrmann, this volume), and its influence on both neutron porosity and resistivity is probably minor.

The Beacon Sandstone shows a very homogeneous electrical resistivity. The highest resistivities were found in the doleritic shear zone from 780 to 820 mbsf, indicating low porosities in this depth interval. Over the entire Tertiary section of the borehole, resistivity shows a highly varying character with peaks and differing baselines. In particular below 440 mbsf, the peaks in the resistivity curves can be clearly attributed to conglomerates. In the uppermost part down to 100 mbsf, resistivity continually increases due to sediment compaction. From 100 to 200 mbsf the resistivity baseline is high, with several peaks up to 500 ohm·m. The section from 200 to 440 mbsf is characterized by alternating resistivities, also showing high values for muddy sections (*i.e.*, at 308 – 316 mbsf). The lowest resistivity baseline is found from 440 to 630 mbsf with again high values for conglomerates and lonestones. Similar to susceptibility and magnetic anomaly baselines, the resistivity baseline is relatively high from 630 mbsf to the top of the doleritic shear zone. In general, the electrical resistivity curve reflects the porosity, but the resistivity baseline may indicate differences in the formation factor and thus in sediment source.

## DENSITY, NEUTRON POROSITY AND VELOCITY

Density logs were obtained for the open-hole NQ part of the hole, whereas through-pipe logs were run in the HQ part (above 345 mbsf). The through-pipe density values were corrected by comparing average density values in the 100 m above and below the

change from NQ to HQ drillstring. The whole-core density logs demonstrate that the average densities for these two intervals are about the same. In general, core and log measurements of bulk density are consistently very similar, indicating that both are reliable. No systematic difference between bulk density core and log measurements was observed, showing that there was no measurable stress release in the cores.

The raw neutron log is a ratio of counts measured by a far ($phi_{long}$) and a near ($phi_{short}$) detector. To make the measured neutron porosities comparable to formation porosity, a porosity log (poro) was calculated from the measured counting ratio of the neutron porosity tool derived from cross correlation with core-derived porosities using the following formula:

$$poro = 22 + 31.7 \ln(phi_{long}/phi_{short}).$$

Initially, the HQ interval (above 345 mbsf) was logged open-hole with the neutron tool. During the third logging phase, this interval was relogged through-pipe, and this latter log is presented here. The two logs show a very high correlation. Only a slight pipe effect appears to be present, but this is so small that no pipe correction was applied. However, the relationship between porosity and the ratio of countrates from long and short detector is not linear resulting in higher errors at high porosities.

Neutron porosity measures the total hydrogen content of the formation, including water bound in clays plus free water in pores. Thus, neutron porosities can be too high in formations that are rich in clay minerals. On the other hand, this effect can be used in combination with density measurements to determine clay content and clay type (Bücker et al., 2000b). The downhole porosity log shown in figure 1 was corrected to core porosity by using the formula given above.

The sonic velocity tool was the only tool that did not provide a good quality log. This tool measures p-wave velocity based on picked travel-times of refracted waves from a sound source to two receivers. The strength of this refracted wave was generally too weak to be reliably detected by the far source-receiver combination. After returning home we recognised that this weak signal was due to a tool failure. Because of the high mud salinity, the material of the receivers was swollen and this obscured the received signal. The velocity log shown here (Fig. 1) was measured on cores and is thus indicated by 'c'.

Down to 100 mbsf, the porosities show a compaction trend. Below this depth, the porosities show a good correlation with the neutron, density and core-derived sonic-velocity logs. The highest velocities and densities and, accordingly, lowest porosities were found for the doleritic conglomerate from 780 to 820 mbsf. Conglomerates can be clearly detected by their high velocities of up to 6 km/s and densities up to 2.6 g/cm$^3$. Average velocity in the lowermost sedimentary section from 630 – 780 mbsf is about 3.7 km/s. In general, velocities in CRP-3 are about 3.2 ± 0.6 km/s, apart from the first 100 m of core, where velocity is less than 2.0 km/s, and the dolerite shear and conglomerate zone, where velocity is greater than 4.5 km/s. The average velocity for the CRP-3 core is much lower than previously thought (Bücker et al., 1998). Cooper & Davey (1987) used stacked velocities from reflection seismic processing. This finding has a considerable effect on the interpretation of the offshore seismics of the entire Ross Sea and is discussed in detail by Henrys et al. (this volume).

Porosity is the dominant variable affecting neutron porosity, density, sonic velocity, and resistivity. Therefore, these logs are often referred to as porosity logs. Porosities of most siliclastic sediments depend on grain size and compaction history. Sea-floor porosities of well-sorted sands are about 30 – 40 %, whereas clays show porosities of up to 80 % or more (*e.g.*, Hamilton, 1971). Initial porosities are subsequently decreased both by mechanical compaction and by chemical diagenesis. The carbonate content, which is the main cementation mineral in the CRP-3 core, is discussed by Dietrich (this volume).

Small-scale variations in both the sgr and magnetic susceptibility logs show a positive correlation with variations in density and electrical resistivity throughout most of the Tertiary sediments. This relationship is similar to that commonly seen for highly compacted sandstones and shales. Silty and muddy beds are less porous, higher in density and velocity, and higher in both radioactive elements and magnetic minerals than are sandy beds. Comparison with the core-derived lithology log confirms that this predicted lithological association is present.

Figure 1 shows plots of three porosity-sensitive downhole logs resistivity, density, and velocity. As expected, the broad trends in all three logs are very similar, except for a gradual decrease in resistivity, which is expected to occur independently of porosity change. Rock resistivity depends on both porosity and pore-fluid resistivity. Pore-fluid resistivity decreases gradually downhole due to the thermal gradient, causing an associated downhole decrease in observed formation resistivities that is superimposed on the pattern of porosity changes.

The changes in neutron porosity, resistivity, velocity and density with depth do not follow a simple compaction trend often found in siliclastic sediments (Hamilton, 1976). No systematic depth-dependent decrease in porosity is evident below 200 mbsf. This finding for the CRP-3 drillhole differs from the strong downhole porosity decreases observed in CRP-1 (Niessen & Jarrard, 1998) and CRP-2 (Brink et al., 2000). Apparently, diagenesis and grain-size fluctuations affect present porosity much more than the early mechanical compaction and cementation

history does (Jarrard et al., this volume; Jarrard et al., 2000; for $CaCO_3$ content see Dietrich, this volume).

Table 1 gives average values for the physical properties of some lithological units in CRP-3 with the highest values for each property shown in bold print. The mudstone from the depth section 125 - 140 mbsf, which is below the compaction-influenced first 100 m of the core, shows the highest susceptibility and magnetic anomaly values. The porosity is also very high (24 %). The Beacon Sandstone from 825 to 900 mbsf has considerably different physical properties than other sandstones, *i.e.* in the depth sections 185 - 200 mbsf, 480 - 510 mbsf and 645 - 660 mbsf. In particular, the porosity is markedly lower in the Beacon Sandstone (7 %), although densities and velocities are comparable. However, due to the distinctly lower porosity and somewhat higher velocity, seismic offshore measurements should clearly detect the Beacon Sandstone. The other three sandstones can be clearly distinguished by their physical properties. Sandstone I, in the depth section 185 - 210 mbsf, has the highest resistivity; sandstone II, in the depth section 480 - 510 mbsf, has the lowest magnetisation; and sandstone II, in the depth section 645 - 660 mbsf, has the highest susceptibility.

## VISUALLY DERIVED LOG-BASED UNITS

In the Initial Report on CRP-3 (Cape Roberts Science Team, 2000), the interval 0 - 901 mbsf was divided into five logging units on the basis of logs. After full processing of the downhole logging data set, the changes to the limits of these logging units are only minor.

Log Unit I, 0 - 144 mbsf, is characterised by generally very homogeneous log responses, particularly for the gamma-ray, magnetic susceptibility, and K/Th logs. Resistivity, density and velocity show a downward increase, whereas porosity generally decreases. There is no clear response for the diamictites (*i.e.*, 85 - 95 mbsf), possibly due to high mud content.

Log Unit II, 144 - 630 mbsf, is characterised by bimodal responses for all the logs, with one mode similar to log Unit I. Alternations on a 10 – 30 m scale are due to sedimentary sequences (Naish et al., this volume). A basal conglomerate marks most sequence boundaries with high resistivity and density, low porosity, and high susceptibility and magnetic values. The gamma ray responses of the conglomerates change downhole from low to higher values, and the characteristic low K/Th signature becomes more evident downhole. The conglomerates are clearly seen as spikes on the resistivity curve, because of the combination of poor sorting and high cementation. Some fining upward sequences from clean sand to muddy sand and silt are visible in the log responses.

Log Unit III, 630 - 790 mbsf, is lithologically relatively homogeneous, with low gamma-ray values, but enhanced Th/K values and high susceptibilities and magnetisation. Porosity, density, and velocity are heterogeneous, with variations similar to those in log Unit II: low porosities in the conglomerates and well-cemented sandstones, with high-porosity sandstones also present. Except for the conglomerates, grain-size changes are not as evident in the gamma ray and susceptibility logs as in log Unit II. This finding is consistent with core descriptions of this unit as mostly greenish sandstone. Fining and coarsening upward sequences are also seen in the susceptibility and gamma ray logs.

Log Unit IV, 790 - 823 mbsf, is characterized by very low porosities, very high susceptibilities, and relatively low gamma ray values. This unit consists of a fault zone (790 - 803 mbsf), with elevated gamma-

*Tab. 1* - Average values for the physical properties of some characteristic lithological units in CRP-3 (abbreviations see figure caption of figure 1). The highest values for each property are shown in bold. The mudstone from 125 – 140 mbsf shows the highest porosity values. The Beacon Sandstone from 825 – 900 mbsf has considerably different physical properties than the other three sandstones, *i.e.*, in the depth sections 185 – 200 mbsf, 480 – 510 mbsf, and 645 – 660 mbsf. The porosity is markedly lower in the Beacon Sandstone. Thus, seismic measurements should clearly detect the Beacon Sandstone. Sandstones II and III show nearly the same thorium/potassium ratio, but their susceptibility values are distinctly different. Density measurements could not be made for the igneous intrusion below 900 mbsf due to material falling to the bottom of the hole (n.v.: no values).

| **Lithology** | **clay** | **sand-stone I** | **sand-stone II** | **sand-stone III** | **Beacon Sandstone** | **Igneous Intrusion** |
|---|---|---|---|---|---|---|
| **Depth (mbsf)** | **125-140** | **185-200** | **480-510** | **645-660** | **825-900** | **900-910** |
| K (%) | 2 | 2 | 1 | 1 | 3 | **4** |
| U (ppm) | 2 | 2 | 1 | 1 | 2 | **3** |
| Th (ppm) | 7 | 6 | 2 | 3 | **11** | 5 |
| Th/K | 3.5 | 3.2 | 1.8 | 1.5 | **4.1** | 1.5 |
| Rdeep (Ohmm) | 8 | **17** | 4 | 8 | 7 | 6 |
| sus ($10^{-3}$ SI) | 25 | 23 | 3 | **28** | 0 | 4 |
| delta_z (nT) | **-80** | 60 | -10 | 10 | 0 | -4 |
| rho (g/cm$^3$) | 2.2 | 2.3 | **2.4** | **2.4** | **2.4** | n.v. |
| poro (%) | **24** | 19 | 20 | 22 | 7 | 19 |
| vpc (km/s) | 2.8 | 3.2 | 2.6 | 3.1 | **3.3** | 2.7 |

ray values and the highest susceptibility values of the entire borehole, and Tertiary doleritic sediments (803 - 823 mbsf).

The transition from log Unit IV to V is very sharp and corresponds to the major unconformity between Tertiary and Devonian sedimentary rocks.

Log Unit V, 823 - 901 mbsf, is the upper part of the Beacon Sandstone. As mentioned earlier, the Beacon Sandstone is non-magnetic, visible in the susceptibility and magnetic anomaly logs. Porosity is higher than in the overlying doleritic conglomerate but lower than in the entire Tertiary section of the hole. The gamma ray log shows a remarkable variation in the Beacon Sandstone, with lower values in the upper part and the highest values in the lower part, dividing the Beacon Sandstone at about 855 mbsf into two parts. The high gamma ray values are supported mainly by elevated thorium and potassium contents. These high values are incompatible with expectations based on the mineralogical maturity of analogous Beacon outcrops, suggesting that diagenetic precipitation has enriched these sandstones in K and Th. For detailed listings of the physical properties in the log units see also table 1.

Unfortunately, because of bridges and material falling to the bottom of the borehole, only a few values could be obtained for the igneous intrusion below 900 mbsf.

It was time intensive to derive these visually identified logging units; they are very subjective and depend mainly on the observer's experience. Objective statistical methods are faster and much more reliable and better suited to establish logging units (Bücker et al., 2000) and are described in the following sections.

## APPLICATION OF MULTIVARIATE STATISTICAL METHODS

The multivariate statistical procedure used in the evaluation and interpretation of the downhole logs is described in detail by Bücker et al. (2000a). The CRP-3 downhole logs were treated similar to the CRP-2/2A logs. The data set has to be prepared prior to the factor and cluster analyses. The first step is an intensive quality control and editing of spikes *etc.* from the entire data set. The next step consists of filling all gaps in the downhole measurements data set by cross correlation with other physical property data that do not have gaps. Gaps in the electrical resistivity and magnetic susceptibility curves, which could not be measured through the drillpipe, were filled by correlation with the downcore velocity log (correlation coefficient R in the depth section 150 – 350 mbsf: R = 0.57, and R = 0.65, respectively). The magnetic anomaly log delta_z was filled by correlation with the susceptibility log (R = 0.65). The next data preparation step consisted of a test for normal, *i.e.*, Gaussian distribution within each data set. Electrical resistivities and magnetic susceptibilities exhibit a log-normal distribution, and an application of a logarithmic transform to these logs yielded observations that are normally distributed.

Finally, the observational data were standardised by subtracting the mean and dividing by the standard deviation. The resulting logs are dimensionless, each with a mean of zero and a standard deviation of 1. This procedure permits comparison of all the original downhole logs, regardless of their original scaling.

### FACTOR LOGS

With factor analysis, interrelationships among a set of variables are examined. This technique is used to derive a subset of uncorrelated variables called factors that explain the variance in the original observational data set without losing important information. With this procedure, the dimensionality of the original data set is reduced, resulting in two or three factors that account for nearly all the variance in the original data set. This makes the interpretation of the huge amount of logging data much simpler, as the factor logs respond to important sedimentological features such as grain size, provenance or glacial influence (Bücker et al., 2000b).

Factors and factor loadings were calculated from the standardised logging curves using standard R-mode factor analysis procedures (Davis, 1986; Backhaus et al., 1986; Tabachnick & Fidell, 1991). A Kaiser Varimax factor rotation of the matrix of factor loadings resulted in a simplification of the factor co-ordinate system. The resulting factor model is simply a linear combination of underlying physical and/or chemical properties. A factor is taken as being significant for an underlying property, if its eigenvalue is greater than 1. Theoretically, the factor logs are uncorrelated. This is not always the case, because the borehole geophysical tools were initially designed to respond primarily to porosity and lithology (Elek, 1990). Consequently, the first two factors derived from the factor analysis are also related to porosity and lithology.

One of the main advantages of the factor logs is that they are - by definition - not interrelated. The ambiguity of the downhole logs is strongly reduced and the factor logs can be interpreted directly in terms of the controlling background variables. However, as the rock properties themselves are not uncorrelated in all cases, some correlation between the factor logs is possible.

All of the downhole logs of figure 1 were included in the factor analysis of the Tertiary section of the hole down to 790 mbsf. Only the shallow resistivity was not used because it shows a strong correlation with the parameter RDeep. For this data set, 76 % of the variance observed in the input variables can be described by the first three factors,

although the number of variables has been reduced from 11 to 3. This means that the factor extraction resulted in a reduction of the logs by a factor of four, whereas more than three-quarters of the original information is kept. The results of the factor analysis, together with communalities, factor eigenvalues and factor loadings, are listed in table 2. The factor logs are displayed in figure 2, together with the lithology column, the gamma ray and magnetic susceptibility logs and the multivariate cluster log. The clear grouping of variables (Tab. 2) and different patterns of the factor logs (Fig. 2) confirm that in this case, the relationship between factors and shared background information is negligibly small.

Factor loadings greater than ± 0.5 are taken as significant and shown in bold print in table 2.

*Tab. 2* - Results of factor analysis of downhole logs from CRP-3. The number of valid cases is the number of values in each downhole log used for the analysis. The upper part of the Table presents communalities, eigenvalues and proportion of explained variance. The eigenvalues are assumed to be significant if they are greater than or equal to 1; these are in bold print here, shown in figure 2, and included in the subsequent cluster analysis. The lower part of the Table gives the factor loadings, the communality, and the total amount of explained variance. Factor loadings greater than 0.5 are shown in bold. The sum of the factor loadings squared is equal to the eigenvalue, which is the variance explained by a factor. Three factors have an eigenvalue greater than 1. The total variance explained by these three factors is 76%. (An explanation of the variables is given in Figure 1.) Factor 1 and Factor 2 show nearly the same percentage of explained variance (30%).

**Factor Analysis** valid cases: 769

**Communalities**

| | estimated | Analysis |
|---|---|---|
| sgr | 1 | 0.960 |
| K | 1 | 0.847 |
| U | 1 | 0.573 |
| Th | 1 | 0.883 |
| rho | 1 | 0.819 |
| poro | 1 | 0.629 |
| Vpcore | 1 | 0.841 |
| delta_z | 1 | 0.624 |
| logRDeep | 1 | 0.803 |
| logsus | 1 | 0.726 |
| ThK | 1 | 0.654 |

**Eigenvalues**

| Factor | Eigenvalue | Variance Percent | Percent cumulated |
|---|---|---|---|
| **1** | **3.72** | **33.82** | **33.82** |
| **2** | **3.43** | **31.20** | **65.03** |
| **3** | **1.21** | **10.99** | **76.01** |
| 4 | 0.84 | 7.66 | 83.67 |
| 5 | 0.54 | 4.88 | 88.55 |
| 6 | 0.41 | 3.73 | 92.28 |
| 7 | 0.30 | 2.73 | 95.01 |
| 8 | 0.23 | 2.11 | 97.12 |
| 9 | 0.17 | 1.55 | 98.66 |
| 10 | 0.11 | 1.01 | 99.68 |
| 11 | 0.04 | 0.32 | 100.00 |

**Varimax Factor Loadings**

| | Factor 1 | Factor 2 | Factor 3 | communality |
|---|---|---|---|---|
| **sgr** | **0.96** | -0.08 | 0.20 | 0.96 |
| **K** | **0.90** | -0.03 | -0.18 | 0.85 |
| **Th** | **0.83** | -0.12 | 0.42 | 0.88 |
| **U** | **0.75** | -0.02 | 0.13 | 0.57 |
| **Vpc** | -0.03 | **0.91** | 0.12 | 0.84 |
| **logRDeep** | 0.17 | **0.84** | 0.26 | 0.80 |
| **rho** | -0.39 | **0.82** | 0.02 | 0.82 |
| **poro** | 0.04 | **-0.78** | 0.16 | 0.63 |
| **ThK** | 0.12 | -0.10 | **0.79** | 0.65 |
| **logsus** | 0.37 | 0.34 | **0.69** | 0.73 |
| **delta_z** | -0.13 | **0.54** | **0.56** | 0.62 |
| **Square sum** | 3.33 | 3.25 | 1.78 | 8.36 |
| **Percentage of Variance** | 30.30 | 29.55 | 16.16 | **76.01** |

## CLUSTER LOG

In general, cluster analysis is an ideal technique for grouping individuals or samples into *a priori* unknown groups. The objective of the cluster analysis is to form groups on the basis of measured characteristics with the aim of maximising the differences between the groups. The Ward method is the most commonly used method that uses a Euclidean norm for complete-linkage hierarchical clustering (Davis, 1986) and was used in this study. The factor logs were used as input logs for the cluster analysis, and statistical electrofacies were defined. To decide how many clusters are significant and useful, a cluster dendrogram and the so-called elbow criterion were used. The resulting statistical electrofacies, or logging units, which stand for distinct combinations of rock physical and chemical properties (*e.g.*, Serra, 1986; Doveton, 1994), are shown in figure 3. For the CRP-3 site, five significant clusters were obtained for the Tertiary section of the hole down to 790 mbsf on the basis of multivariate analysis of the three factors. Taking more clusters into consideration would simply result into a subdivision of these five clusters, complicating the interpretation. However, it may be helpful for refined interpretation in certain depth sections.

# RESULTS AND DISCUSSION

## FACTOR AND CLUSTER LOGS

The factor analysis shows that the first two factors are equally weighted, and each of them contributes 30 % to the variance. The third factor contributes half of the variance of the first two factors (Tab. 2). The factor analysis revealed the most discriminating variables to be gamma ray, potassium, and velocity, each with a factor loading greater than 0.9. Factor 1 is loaded by the radiogenic properties gamma ray, potassium, thorium, and uranium (Tab. 2). Factor 2 is loaded by the index properties velocity, resistivity, density and porosity, and to a small amount by the magnetisation delta_z. Factor 3 is loaded by the thorium/potassium ratio, the susceptibility and to a small amount also by the magnetisation delta_z.

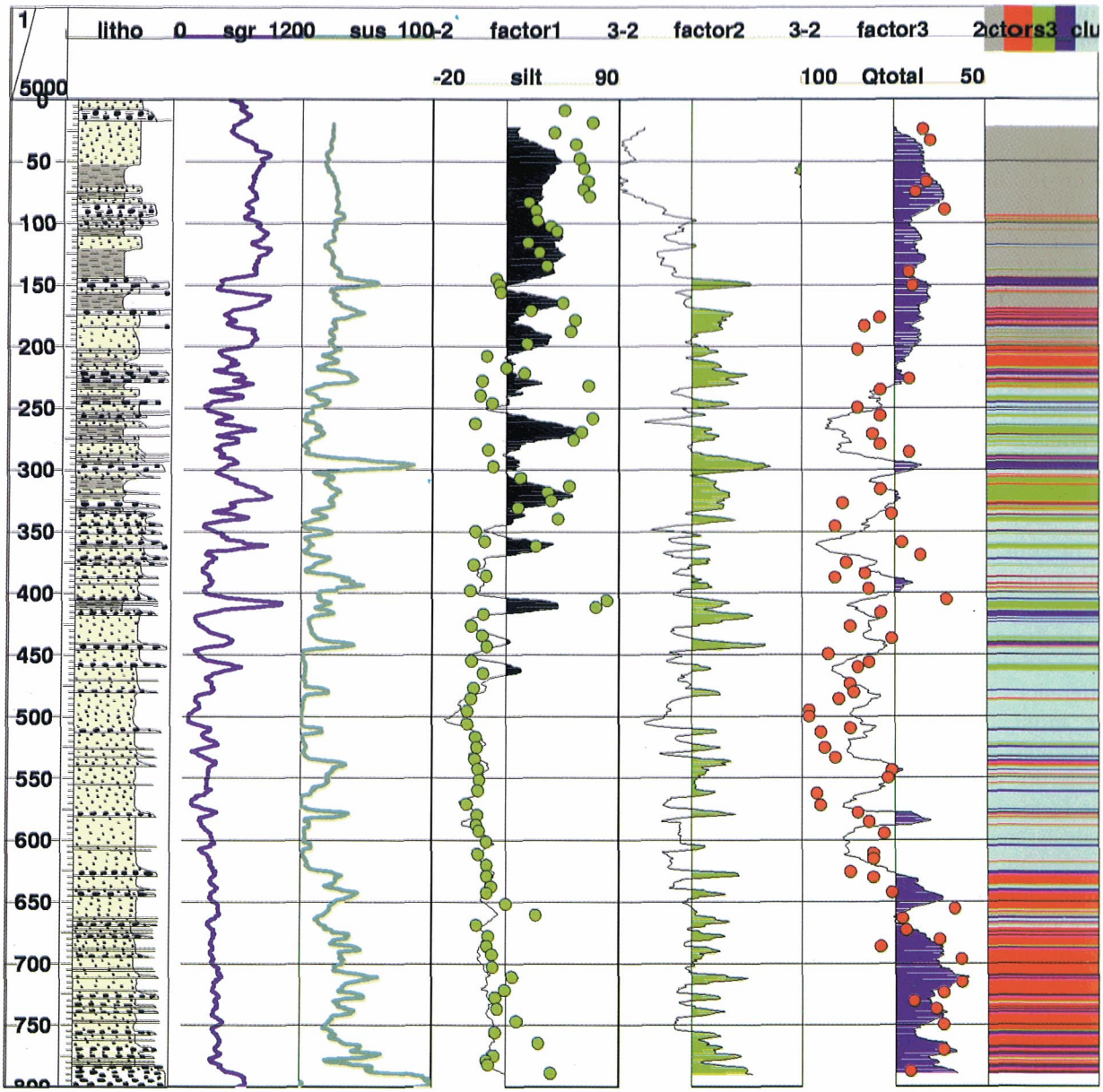


*Fig. 2* - Core-derived lithology, downhole logs for gamma ray (sgr) and susceptibility (sus), factor logs, and cluster log for the Tertiary section of the hole. The downhole logs are the same as in Figure 1. Factor1, Factor2, and Factor3 are the factor logs as derived by factor analysis. Colored areas denote factor values greater than zero. The multivariate cluster log (right column) was calculated on the basis of these three factor logs.

The Factor1 log is mainly related to grain size (high loading of sgr, K, U, Th), whereas the Factor2 log is related to effective porosity (high loading of porosity, density, sonic velocity, resistivity) and, to a lesser extent, to delta_z.

The green dots plotted together with Factor1 represent measurements of silt content by Ehrmann (this volume). Factor2 may be viewed as a glacier and/or ice-rafting indicator, positive values represent conglomerates or diamictites. The Factor3 log (loaded by the ratio Th/K, the susceptibility, and the magnetic anomaly delta_z) indicates sediment source. The red dots (Qtotal) represent the total quartz content derived by Smellie (this volume) on a reversed scale. The observed anticorrelation between factor3 log and quartz content confirms the Factor3 log as provenance proxy. The multivariate cluster log (right column) can be divided into three main sections: 0 – 200 mbsf, 200 – 630 mbsf, 630 – 790 mbsf. The colours represent each of the five clusters (*cf.* Tab. 3). Clusters 1 (grey) and 3 (green) represent two mudstones with different sediment sources, clusters 2 (red) and 5 (blue) represent two different sandstones, and cluster 4 (dark blue) represents mainly conglomerates and to a smaller extent diamictites.

Thorium also contributes to factor 3, but the factor loading is only 0.42. The factor logs are shown in figure 2 down to the base of the Tertiary section of the hole at 790 mbsf, together with a simplified lithology column and the gamma ray and susceptibility logs. The specific loadings of the factor logs lead to the following interpretations.

Gamma ray and susceptibility are influenced indirectly by sediment grain-size distribution, at least for these formations. Thus Factor1 is a good proxy for lithology and grain-size variations (Fig. 2). Fine-grained, mud-dominated lithologies are found in the upper section of the borehole down to about 450 mbsf (black areas in figure 2). No mudstones

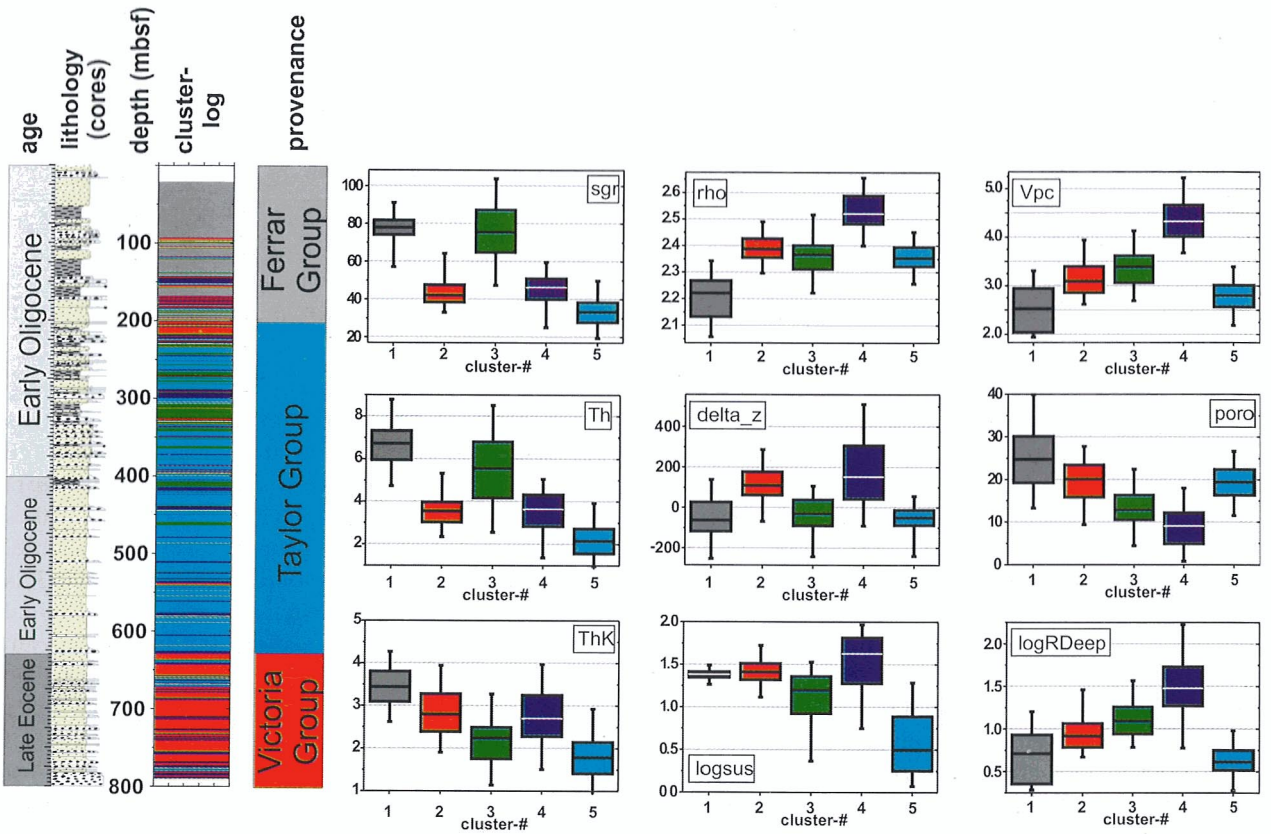


*Fig. 3* - Results of cluster analysis of the downhole logs. The "box-and-whisker" plots show the average values for each parameter in each cluster with 95 % (boxes) and 50 % (whisker) confidence limits. The vertical axis in each diagram is the physical parameter in the corresponding unit. The two sandstones (red and blue) show nearly identical gamma ray, density, and porosity values. But the susceptibility and Th/K ratio differentiates between these two lithological units. The patterns shown in these plots can be viewed as fingerprints of the sediments. From this figure it becomes clearly visible that each cluster (lithological unit) has a characteristic set of physical properties: the fingerprint. For a more detailed interpretation of these fingerprints with respect to sediment source, it is necessary to use reference values of physical properties of rocks from the Transantarctic Mountains, which are not available at the time.

appear below this depth; the lithology consists of sandstones and intercalated conglomerates. In figure 2, the silt content (Ehrmann, this volume) is plotted together with the Factor1 log and shows a good correlation to Factor1 (correlation coefficient 0.58). Only in the uppermost section of the borehole down to 80 mbsf does a noticeable difference occur between Factor1 log and silt content. This difference may be a result of the undercompacted sediments in this depth section. After calibration, the Factor1 log may be viewed as a high-resolution grain-size log. Factor1 is to a smaller extent (-0.39, see Tab. 2) negatively loaded by the density. The negative loading means that there is an anticorrelation with the gamma ray values, which may indicate fine-grained sediments that have a lower density than the coarser grained sediments. But the loading of density to Factor1is only small and may show only a trend for this relation.

Factor2 is loaded by all the physical properties that are influenced by porosity (velocity, density, resistivity, neutron porosity). Thus, the Factor2 log may be viewed as a true porosity log and delineates mainly the low-porosity and high-density conglomerates and to a lesser amount diamictites in the upper portion of the hole. Sections with Factor2 values greater than zero are shaded green in figure 2 and mark the high-density/low-porosity conglomerates and diamictites. Diamictites are often mixed with a considerable amount of clay, thus preventing them from being differentiated from mudstones. The upper part of the borehole down to about 100 mbsf shows very low Factor1 values and porosities, confirming the assumption made for Factor1 that this part is underconsolidated and thus masks the actual physical and chemical properties. As the diamictites and conglomerates are mainly related to glaciers and/or ice rafting, the Factor2 log acts as an ice indicator for climate interpretation. However, as pointed out earlier, it does not seem to be possible to clearly distinguish between diamictites and conglomerates. Factor2 is also loaded by the magnetic properties delta_z and to a smaller extent by the susceptibility, indicating a higher proportion of magnetic minerals, such as magnetite, in the high-density lithologies. Below 144 mbsf presence of diamictites and conglomerates can be clearly detected on the basis of their elevated susceptibility, magnetic anomaly and resistivity values.

*Tab. 3* - Calculated physical properties of clusters of the multivariate cluster analysis shown in Figure 2. Numbers in bold print represent the highest value of the property and illustrate its respective cluster (see Figure 1 for units). Each cluster has a different combination of physical properties. For example, clusters 1 and 3 have identical sgr values, but they have significantly different Th/K ratios and susceptibilities, suggesting different sediment compositions and thus, different rock sources. (An explanation of the variables is given in figure 1).

| cluster # | sgr | K | U | Th | rho | poro | vpc | delta_z | Rdeep | sus | Th/K | lithology |
|---|---|---|---|---|---|---|---|---|---|---|---|---|
| **1 (grey)** | **77** | 2 | **2** | **6.7** | 2.21 | **25** | 2.5 | -55 | 4.7 | 24 | **3.4** | **mudstone 1** |
| **2 (red)** | 44 | 1.3 | 1.1 | 3.6 | 2.39 | 20 | 3.16 | 117 | 9.1 | 25.6 | 3 | **sandstone 1** |
| **3 (green)** | 76 | **2.6** | 1.9 | 5.5 | 2.36 | 13 | 3.36 | -36 | 13.2 | 12.5 | 2.2 | **mudstone 2** |
| **4 (blue)** | 45 | 1.3 | 1.3 | 3.5 | **2.53** | 9 | **4.38** | **179** | **31.6** | **30.1** | 2.7 | **conglomerate** |
| **5 (light blue)** | 34 | 1.2 | 0.8 | 2.2 | 2.36 | 19 | 2.81 | -62 | 4.3 | 3.8 | 1.8 | **sandstone 2** |

Especially below about 440 mbsf, each conglomerate section and even relatively large lonestones are detected by the Factor2 log.

Loading of Factor3 is due mainly to properties that are not directly related to grain size or lithology. The thorium/potassium ratio (Th/K) is independent of the absolute values, which makes this parameter valuable as a sediment source indicator. To a lesser extent, the absolute thorium content also shows a positive correlation with Factor3 (0.42, see table 2). Magnetic susceptibility and magnetic anomaly are parameters, which are influenced by the amount of magnetic minerals like (titano) magnetite series or hematite. The first d emagnetisation tests on CRP-3 samples indicate that magnetite is the predominant magnetic mineral in these specific horizons (Cape Roberts Science Team, 2000). In figure 2, the Factor3 log is plotted together with the total quartz content (Smellie, this volume) on a reversed scale. The observed anticorrelation between the Factor3 log and the total quartz content indicates that Factor3 acts as a provenance indicator. The Tertiary section of the CRP-3 drillhole down to 790 mbsf can be divided according to Factor3 into an upper, middle and lower part (blue areas in figure 2 denote Factor3 values greater than zero). The upper and lower part show high Factor3 values and low quartz contents, whereas the middle part is characterized by low Factor3 values and higher and varying quartz contents. As the uppermost section of the borehole is dominated by mudstones, the low quartz content is reasonable. But the low quartz content in the section from 630 – 790 mbsf, where sandstones are observed that are similar to the sandstones above this section, the high Factor3 values and low quartz contents indicate a different sediment source. Following this interpretation, the Factor3 log acts as a provenance proxy, and is not just reflecting mud content.

The multivariate clusterlog was calculated by using the three factor logs as input variables (right column in figure 2). The advantage of using the three factor logs instead of the eleven downhole logs is the reduction of variability and fine scale variations, which could complicate interpretation. The mean and standard deviation of the calculated physical properties of each cluster are given in table 2 and graphically presented in figure 3 as so-called box-and-whisker plots. The different physical properties represented by the clusters are depicted as average values with 95 % (boxes) and 50 % (whisker) confidence limits. This graphical representation makes the grouping of physical properties clearly visible. The arrangement of the coloured boxes in figure 3 is characteristic for each cluster and acts as a physical fingerprint for the drilled sediments. By dendrogram evaluation, five clusters were derived as characteristic of the Tertiary section of the hole. Taking more clusters into account would result in a subdivision of the five cluster solution and might be helpful for observations at finer depth scales, but would complicate the general interpretation. Each cluster has a different combination of physical properties and can be seen as a statistically determined electrofacies or petrofacies as defined by Serra (1986). For example, clusters 1 and 3 (grey and green, respectively, in the cluster log in figure 2) have identical sgr values, suggesting mudstone as the petrofacies. But they have significantly different Th/K ratios and susceptibilities, indicating different sediment compositions and thus different rock sources. The same is true for the two types of sandstones, which are marked in blue and red in the cluster column in figure 2. These two sandstones have comparable radioactive properties and physical properties such as porosity. But the magnetic susceptibility, magnetic anomaly delta_z, and the Th/K ratios are totally different. These source–rock-dependent properties again indicate different sediment sources for these two sandstones in the borehole. Diamictites and conglomerates are marked blue, which represents high index properties, and also the highest magnetic values. The conglomerates apparently consist of rocks enriched in magnetite, which may also indicate a specific rock source in the Transantarctic Mountains.

In general, the cluster log in figure 2 can be divided into three main sections; the first unit is dominated by the grey mudstones down to about 200 mbsf. The blue sandstone is clearly the most prominent feature in the depth section from 200 – 630 mbsf. In the upper portion, this sandstone is intercalated with mudstones (shown in green), which show different properties from the mudstones (shown in grey) in the uppermost section of the borehole. The lowermost Tertiary section of the borehole from 630 –

790 mbsf is dominated by the red sandstone with the higher magnetite component than the blue sandstone. However, some of these red sandstones are also indicated at 200 mbsf depth, which may indicate a short-term change in sediment source at this depth (time).

At the left margin of figure 3, the time scale, simplified core-derived lithology, and the cluster log are shown. In the next column, the cluster log was simplified into three main units. These three main units can be compared to the provenance analysis by Smellie (this volume). An excellent correlation with a Taylor Group sediment source can be seen for the depth section from 200 – 630 mbsf, and with a Victoria Group sediment source from 630 to 790 mbsf. This supports the above assumption that the cluster log mainly summarises rock source information, and to a lesser extent lithology information. The results of the cluster analysis and the relation to sediment provenance can also be compared with some other results. For example, the carbonate distribution (Dietrich, this volume) shows a pattern similar to that of the cluster log. From 0 to 220 mbsf the carbonate content is low, with an average value of about 3 %; between 220 and 630 mbsf it is higher on average and varies between 1% and 10 %; and below 630 mbsf carbonate is again low and fairly constant at 2 %. These different carbonate contents may reflect diagenesis stages and influence the mechanical properties velocity and porosity and also the magnetic properties, since the change at 630 mbsf is not accompanied by a velocity change. This missing sharp velocity change may be due to a more gradual and progressive change in provenance. Detailed magnetic studies (Florindo et al., this volume) yielded results, which fit excellently to the cluster analysis. Magnetic studies on core plugs also showed a change at 630 mbsf with elevated susceptibilities and natural remanent magnetisations. Magnetic hysteresis experiments also detected the change in the grain size of magnetite at 630 mbsf (Sagnotti et al., this volume). These elevated susceptibilities can be related to a change in oxidation conditions and thus to a warmer climate represented by the sediments below 630 mbsf in CRP-3. These elevated susceptibilities can also be related to the $\delta O^{18}$ curve for the southern ocean, indicating the change from Oligocene to Eocene and a warmer climate (Zachos et al., 1996). Clay analysis (Neumann et al., this volume) reveals a higher smectite content below 600 mbsf, again confirming a major change at this depth. The downhole logging results from the CIROS-1 drillhole (Bücker et al. 1998) show that the early Oligocene/late Eocene change is also accompanied by a susceptibility change at about 430 mbsf from lower to higher values (Sagnotti et al., 1998, Wilson et al. 1998,). Summarising all these findings suggests that the early Oligocene/late Eocene boundary is encountered in the CRP-3 drillhole at 630 mbsf.

## COMPARISON WITH SEISMIC STRATIGRAPHY

The cluster log summarises lithological and sediment source information and is thus excellently suited for a comparison with the seismic stratigraphy (see Henrys et al., this volume). The simplified cluster log of figure 3 is shown in figure 4 with the Devonian section added below 790 mbsf down to the bottom of the hole at 939 mbsf together with the seismic stratigraphy of Henrys et al. (this volume). The Ross Sea seismic units V3, V4, and V5 from Cooper & Davey (1987) drilled by the Cape Roberts drillholes CRP-1, CRP-2/2A, and CRP-3 are also shown in figure 4. Drillhole CRP-2/2A crossed the V3/V4 boundary at about 80 mbsf and the V4/V5 boundary at about 440 mbsf. The V4/V5 boundary was not crossed by drillhole CRP-3, but a major seismic reflector was encountered at 200 mbsf in seismic unit V5. The cluster log for drillhole CRP-2A was taken from Bücker et al. (2000b). Most of the seismic reflectors can be correlated with the results of the cluster analyses, but some could not. For example, the change from the blue cluster to the red cluster in CRP-3, which marks two different sandstone types and a major change in sediment source, but not lithology, is not recognised as a seismic reflector. This is comprehensible when compared with Figure 3. There is no major difference in the index properties density and velocity between these two sandstones. Thus there is no seismic impedance contrast and, therefore, no seismic reflector.

A major seismic reflector in between seismic unit V5 was encountered at about 200 mbsf in CRP-3. Cluster analysis identified this reflector as a change in provenance as well as in lithology. The change in lithology from mudstone to sandstone is accompanied by a change in porosity and velocity, resulting in enhanced seismic impedance and thus a seismic reflector. The upper part of the cluster log for drillhole CRP-2A is dominated by values, which represent mudstones. The seismic boundary between seismic units V3 and V4 was crossed at 80 mbsf, and below this depth no more mudstones with specific characteristics shown in black colour were observed. A major change in cluster pattern from black and green-dominated depth sections to blue and red-dominated depth sections is observed at about 300 mbsf. No prominent reflector can be related to this depth, but the depth marks a change in the dip of the seismic reflectors (change to steeper dips) and thus a tectonic and/or glacial event. The seismic boundary at about 400 mbsf in drillhole CRP-2A (seismic sequences V4/V5 boundary) may be related to a change from one sandstone (blue clusters) to another sandstone (red clusters). These two clusters (blue and red for CRP-2A) differ mainly in porosity

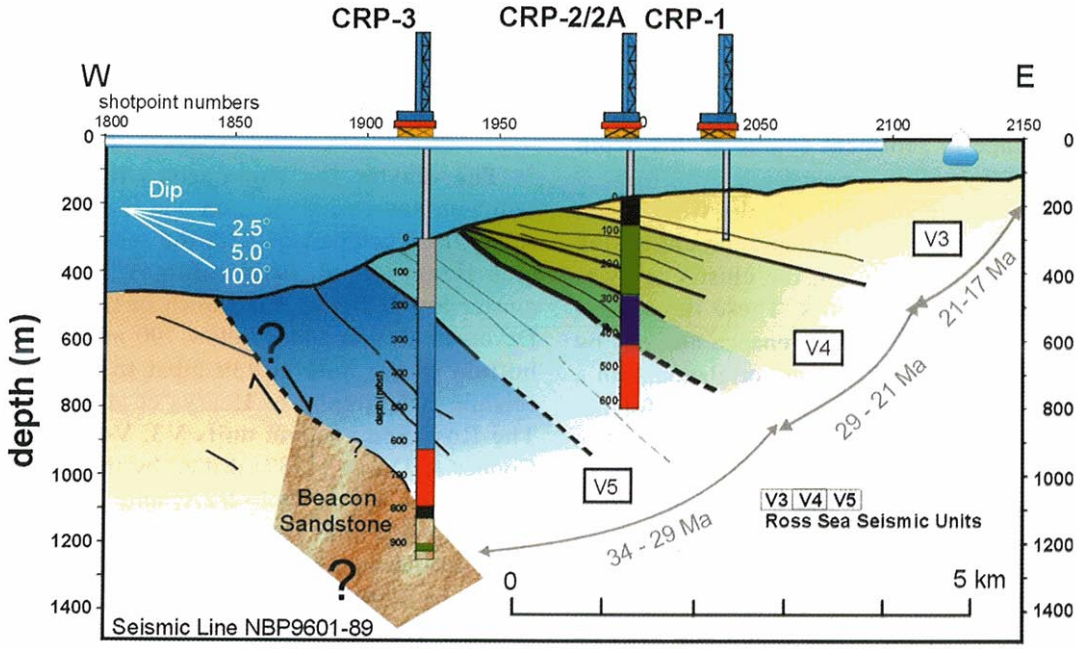


*Fig. 4* - Fit of cluster analysis results into the seismic section (Henrys et al., this volume). The cluster log below the CRP-3 drilling rig is the same as in Figure 3, the cluster column for drillhole CRP-2A was taken from Bücker et al. (2000). Some of the seismic reflectors can be correlated to the cluster analysis but not all of them. For example, the change from the blue cluster to the red cluster in CRP-3, which marks a major change in sediment source, but not lithology, is not seen as a seismic reflector. A major seismic reflector in seismic unit V5 was encountered at about 200 mbsf in CRP-3. Log analysis identified this reflector as a change in provenance as well as lithology. For drillhole CRP-2A a major change in cluster pattern can be observed at about 300 mbsf. No prominent reflector can be related to this depth. But this depth marks a change in the dip pattern of the seismic reflectors and thus a tectonic and/or glacial event. At about 630 mbsf the physical properties of the sediments are changing, this change cannot be identified in a seismic reflector. For the interpretation of seismic line NBP9601-89 see Henrys et al. (this volume). See text for more details.

and velocity, producing the seismic impedance necessary for the seismic reflector.

In summary, it seems reasonable to compare cluster analysis results with seismic stratigraphy. It should be pointed out that seismic analysis is blind to lithological or sediment source changes that are only associated with changes in radioactive or magnetic properties. This is evident for the Ross Sea seismic data and will have consequences for the entire Ross Sea seismic stratigraphy, which has to take into account that sediment properties are not simply reflected by velocity and density.

## CONCLUSION

With the Cape Roberts Project, the most complete and comprehensive set of *in situ* physical properties data has been obtained for Antarctica. The main aim of this paper is a geological interpretation by taking into account all information contained in the measured downhole logs. For this purpose a multivariate statistical procedure is used, which leads to the following results:

The interpretation of the huge amount of logging data is simplified, as the factor and cluster logs respond to important sedimentological features such as grain size, provenance, or glacial influence.

Physical properties of lithological units are clearly and reliably differentiated using cluster analysis.

The basic geological controls (*i.e.* grain size, porosity, clay mineralogy) affecting the measured petrophysical properties are identified using factor analysis, thus making geological interpretations much easier.

Comparison of the clustering results with seismic stratigraphy, and geological correlations with seismic units, link the downhole measurements and lithologies with the seismic lines.

ACKNOWLEDGEMENTS - The Alfred Wegener Institut für Polar- und Meeresforschung, the Bundesanstalt für Geowissenschaften und Rohstoffe, and the German Science Foundation supported this work. Special thanks go to Peter Barrett and Franz Tessensohn for their consistent encouragement, enthusiasm, and helpful discussions. The paper benefited from excellent comments by reviewers Jeroen Kenter and Mike Lovell, many thanks to them! Borehole measurements and their logistics are never simple in these "icy" environments, and we would like to thank everyone who helped make these measurements successful: once more, thanks to Pat Cooper, Alex Pyne, John Alexander, Jim Cowie, and many others at Scott Base and Crary Lab MCURDO, Antarctica. In particular, we would like to thank Peter Schulze (his personal and technical engagement on the ice was exceptional) and Ferdinand Hölscher for their help preparing the downhole measurements equipment for Antarctica.

REFERENCES


Backhaus K., Erichson B., Plinke W. & Weiber R., 1986. *Multivariate Analysemethoden*, **8**, Springer, Heidelberg, 416 p.

Bozzo E., Damaske D., Caneva G., Chiapini M., Ferracioli F., Gambetta M. & Meloni A., 1997. A high-resolution aeromagnetic survey over proposed drill sites off shore of Cape Roberts in the Southwestern Ross Sea (Antarctica). In: Ricci C.A. (ed.), *The Antarctic Region: Geologic Evolution and Processes*, Terra Antartica Publication, Siena, 1129-1133.

Brink J.D., Jarrard R.D., Bücker C.J., Wonik T. & Talarico F., 2000. Sedimentological Interpretation of CRP-2/2A Logs, Victoria Land Basin, Antarctica: Glacial and Sea level Significance. *Terra Antartica*, **7**, 349-360.

Bücker C., Henrys S. & Wonik T., 1998. Revision of the Cenozoic Seismic Velocity Structure of the CIROS-1 Drillhole, Antarctica, and Implications for Further Drilling off Cape Roberts. *Terra Antartica*, **5**, 281-289.

Bücker C.J., Shimeld J., Brückmann W. & Hunze S., 2000a. LWD Data Analysis of Leg 171A: a Multivariate Statistical Approach. - In: Moore, J.C., & Klaus, A. (eds.), *Proceedings ODP, Scientific Results*, **171A**, 1-29 [Online]. <http://www.odp.tamu.edu/publications/171A_SR/VOLUME/CHAPTERS/SR171A02.PDF>

Bücker C.J., Jarrard R.D., Wonik T. & Brink J.D., 2000b. Downhole Logging Data Analysis of Cape Roberts Drillhole CRP-2A: a Multivariate Statistical Approach. *Terra Antartica*, **7**, 299-310.

Bücker CJ., Jarrard R.D. & Wonik T, 2001. Downhole temperature, radiogenic heat production, and heat flow from the CRP-3 Drillhole, Victoria Land Basin, Antarctica. This volume.

Cape Roberts Science Team, 1998. Studies from the Cape Roberts Project, Ross Sea, Antarctica, Initial Report on CRP-1. *Terra Antartica*, **5**, 1-187.

Cape Roberts Science Team, 1999. Studies from the Cape Roberts Project, Ross Sea, Antarctica, Initial Report on CRP-2/2A. *Terra Antartica*, **6**, 1-173.

Cape Roberts Science Team, 2000. Studies from the Cape Roberts Project, Ross Sea, Antarctica, Initial Report on CRP-3. *Terra Antartica*, **7**, 1-180.

Cooper A.K. & Davey F.J., 1987. The Antarctic continental margin: geology and geophysics of the western Ross Sea. *Circumpacific Council on Economic and Mineral resources Earth Science Series*, **5B**. Houston, Circumpacific Council for Energy and Mineral resources. 253p.

Davis J.C., 1986. *Statistics and Data Analysis in Geology, 2nd edn.* Wiley, New York, 646 p.

Dietrich H.-G., Klosa D. & Wittich C., 2001. Carbonate content in CRP-3 drillcore, Victoria Land Basin, Antarctica. This volume.

Doveton J.D., 1994. *Geologic Log Analysis Using Computer Methods, American Association Petroleum Geology Computer Applications in Geology* **2**, 169 p.

Ehrmann W., Smellie J.L. & Talarico F., 2001. Provenance and climate from petrology for CRP-3 - Introduction. This volume.

Ehrmann W., 2001. Variations in smectite content and crystallinity in sediments from CRP-3, Victoria Land Basin, Antarctica. This volume.

Elek I., 1990. Fast porosity estimation by principal component analysis. Geobyte, **5**, 25-34.

Erickson S.N. & Jarrard R.D., 1998. Porosity/formation factor relationships for high-porosity siliclastic sediments from Amazon Fan. *Geophysical Research Letters*, **25**, 2309-2312.

Florindo F., Wilson G.S., Roberts A.P., Sagnotti L. & Verosub K.L., 2001. Magnetostratigraphy of late Eocene - early Oligocene strata from the CRP-3 core, Victoria Land Basin, Antarctica. This volume.

Hamilton E.L., 1971. Elastic properties of marine sediments. *Journal of Geophysical Research*, **76**, 579-604.

Hamilton E.L., 1976. Variations of density and porosity with depth in deep-sea sediments. *Journal of Sedimentary Petrology*, **46**, 280-300.

Henrys S.A., Bücker C.J., Niessen F. & Bartek L.R., 2001. Correlation of seismic reflectors with the CRP-3 drillhole, Victoria Land Basin, Antarctica. This volume.

Jarrard R.D., Niessen F., Brink J.D. & Bücker C., 2000. Effects of Cementation on Velocities of Siliclastic Sediments. *Geophysical Research Letters*, **27**, 593-596.

Jarrard R.D., 2001. Petrophysics of core plugs from CRP-3 drillhole, Victoria Land Basin, Antarctica. This volume.

Naish T.R., Barrett P.J., Dunbar G.B., Woolfe K.J., Dunn A.G., Henrys S.A., Claps M., Powell R.D. & Fielding C.R., 2001. Sedimentary cyclicity in CRP drillcore, Victoria Land Basin, Antarctica. This volume.

Neumann M. & Ehrmann W., 2001. Mineralogy of sediments from CRP-3, Victoria Land Basin, Antarctica, as revealed by X-ray diffraction. This volume.

Niessen F. & Jarrard R.D., 1998. Velocity and porosity of sediments from CRP-1 drillcore, Ross Sea Antarctica. *Terra Antartica*, **5**, 299-310.

Rider M.H., 2000. *The Geological Interpretation of Well Logs*. 2nd ed., Whittles Publishing, Caithness, 280 pp.

Sagnotti L., Florindo F., Verosub K.L., Wilson, G.S. & Roberts A.P., 1998. Environmental magnetic record of Antarctic palaeoclimate from Eocene-Oligocene glaciomarine sediments, Victoria Land Margin. *Geophysical Journal International*, **134**, 653-662.

Sagnotti L., Verosub K.L., Roberts A.P., Florindo F. & Wilson G.S., 2001. Environmental magnetic record of the Eocene-Oligocene transition in CRP-3 drillcore, Victoria Land Basin, Antarctica. This volume.

Serra O., 1986. *Fundamentals of Well-Log Interpretation (Vol. 2): The Interpretation of Logging Data*. Devision Petroleum Sciences., **15B**, 371 p.

Smellie J.L., 2001. History of Oligocene erosion, uplift and unroofing of the Transantarctic Mountains deduced from sandstone detrital modes in CRP-3 drillcore, Victoria Land Basin, Antarctica. This volume.

Tabachnick B.G. & Fidell L.S., 1991. *Using Multivariate Statistics*. Harper and Row, San Francisco, 746 p.

Waxman M.H. & Smits L.J.M., 1968. Electrical conductivities in oil-bearing shaly sands. *Transactions American Institute Mechanical Engineers*, **243**, 107-122.

Wilson G.S., Roberts A.P., Verosub K.L., Florindo F. & Sagnotti L., 1998. Magnetobiostratigraphic chronology of the Eocene-Oligocene transition in the CIROS-1 core, Victoria Land margin, Antarctica: Implications for Antarctic glacial history. *Geological Society of America Bulletin*, **110**, 35-47.

Zachos J.C., Quinn T.M. & Salamy K.A., 1996. High-resolution Deep-Sea Foraminiferal Isotope Records of the Eocene-Oligocene Climate Transition. *Palaeoceanography*, **11**, 256-266.